Influence of Thioketo Substitution on the Properties of Uracil and Its Noncovalent Interactions with Alkali Metal Ions: Threshold Collision-Induced Dissociation and Theoretical Studies†

Zhibo Yang and M. T. Rodgers*

Department of Chemistry, Wayne State University, Detroit, Michigan 48202

Received: August 26, 2005

Experimental and theoretical studies are carried out to determine the influence of thioketo substitution on the properties of uracil and its noncovalent interactions with alkali metal ions. Bond dissociation energies of alkali metal ion−thiouracil complexes, M^+(SU), are determined using threshold collision-induced dissociation techniques in a guided ion beam mass spectrometer, where $M^+ = Li^+$, Na^+, and K^+ and SU = 2-thiouracil, 4-thiouracil, 2,4-dithiouracil, 5-methyl-2-thiouracil, and 6-methyl-2-thiouracil. Ab initio electronic structure calculations are performed to determine the structures and theoretical bond dissociation energies of these complexes and provide molecular constants necessary for thermodynamic analysis of the experimental data. Theoretical calculations are also performed to examine the influence of thioketo substitution on the acidities, proton affinities, and A::SU Watson−Crick base pairing energies. In general, thioketo substitution leads to an increase in both the proton affinity and the acidity of uracil. 2-Thio substitution generally results in an increase in the alkali metal ion binding affinities but has almost no affect on the stability of the A::SU base pair. In contrast, 4-thio substitution results in a decrease in the alkali metal ion binding affinities and a significant decrease in the stability of the A::SU base pair. In addition, alkali metal ion binding is expected to lead to an increase in the stability of both single-stranded and double-stranded nucleic acids by reducing the charge on the nucleic acid in a zwitterion effect as well as through additional noncovalent interactions between the alkali metal ion and the nucleobases.

Introduction

The properties and chemical interactions of thiouracils are of great interest as a result of their biological, pharmacological, and spectroscopic activities. For example, a variety of thiouracils including 2-thiouracil, 4-thiouracil, 2,4-dithiouracil, and 5-methyl-2-thiouracil have been identified as minor components of t-RNA and peptide nucleic acids.[1−3] Studies have shown that the inappropriate replacement of uracil by a thiouracil can be responsible for misrecognition in m-RNA.[4] Thiouracils and a variety of their alkyl and amino derivatives have also demonstrated pharmacological activities.[1,5−20] For example, 2-thiouracil and 4-thiouracil have been used as anticancer and antithyroid drugs[1,5,6] and for the treatment of heart disease.[7,8] Similarly, 6-methyl-2-thiouracil has also been employed as an effective antithyroid drug.[9] In addition, a series of derivatives of 2-thiouracil and 4-thiouracil have demonstrated anticancer,[10] antitumor,[11,12] antithyroid,[13,14] anti-HIV,[15] anti-HBV,[16] and anestethic[17] activities, as well as radioprotective effects against chromosomal damage.[18] Additionally, complexes of transition metal ions with thiouracil derivatives have been shown to exhibit anticancer and antimicrobial activity.[19,20] Thus, the properties and characteristics of thiouracils are of great interest in pharmaceutical research and applications.

Thiouracils have also been employed in various analytical applications, e.g., determination of metal ions such as copper, silver, mercury, and platinum.[21,22] The thioketo groups are "soft" and therefore act as very good ligands for transition metal ions, exhibiting both strong and selective binding.[23,24] In addition, the thioketo group exhibits strong absorption bands in the visible region that can be employed for the detection of thiouracils or transition metal−thiouracil complexes. Thus, the properties and characteristics of thiouracils are also of general chemical interest and analytical utility.

In addition to the pharmaceutical and spectroscopic reasons for examining metal ion interactions with thiouracils, participation of metal ions in biological processes is well known. The presence of metal ions may influence the conformational behavior and function of DNA and RNA. Metal ions are of supreme importance in determining which structures nucleic acids assume as well as the way in which they pack together.[25] Alkali metal ions, and other hard metal ions, have a low tendency to form covalent bonds and are therefore relatively nonspecific binders. Their primary influence is to neutralize the negative charges on the phosphate backbone, thereby stabilizing the double helix.[26−29] Their interaction with the nucleobases also neutralizes the negative charges on the phosphate backbone in a zwitterion effect.[30] Metal ions that bind to the nucleobases generally cause more profound effects on the conformation of DNA and RNA[31] than metal ions that bind to the phosphate backbone. Thus, interaction of metal ions with the nucleobases may provide supporting and fundamental information relevant to biology, chemistry, and pharmacology.

A major focus of our recent work involves application of quantitative threshold collision-induced dissociation (CID) methods to obtain accurate thermodynamic information on metal−ligand systems of biological and pharmaceutical relevance.[32−37] These data also provide absolute anchors for metal

† Part of the special issue "William Hase Festschrift".

* To whom correspondence should be addressed.

10.1021/jp054849j CCC: $33.50
Published on Web 10/19/2005

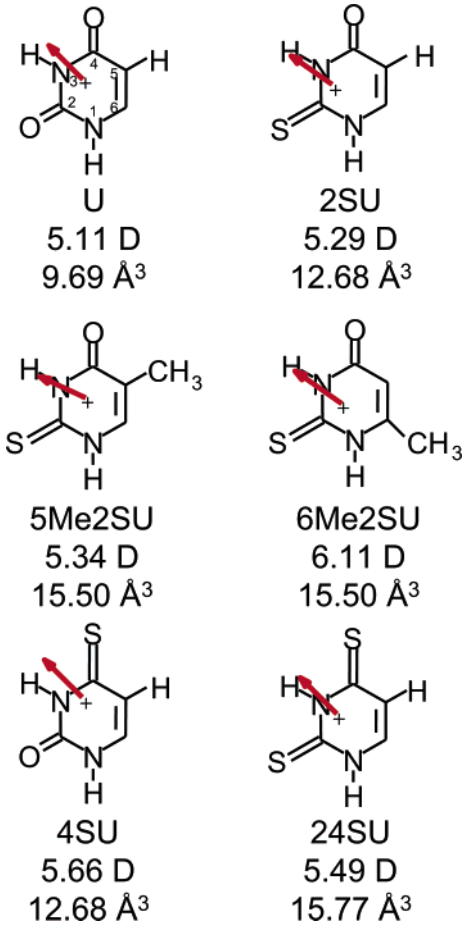

Figure 1. Structures of uracil (U) and the thiouracils (SU). Properly scaled and oriented dipole moments in Debye are shown for each as an arrow. Values for dipole moments are determined from theoretical calculations performed here. The estimated polarizabilities are also shown.[38]

cation affinity scales over a broadening range of energies and ligands. In the present paper we examine the interactions of five thiouracils, 2-thiouracil (2SU), 5-methyl-2-thiouracil (5Me2SU), 6-methyl-2-thiouracil (6Me2SU), 4-thiouracil (4SU), and 2,4-dithiouracil (24SU), with the alkali metal ions Li^+, Na^+, and K^+. The structures of the neutral thiouracils are shown in Figure 1 along with their calculated dipole moments and estimated polarizabilities.[38] Our study utilizes guided ion beam mass spectrometry to measure the cross sections for CID of 15 alkali metal ion−thiouracil complexes with Xe. The kinetic-energy-dependent CID cross sections are analyzed using methods developed previously[39] that explicitly include the effects of the internal and translational energy distributions of the reactants, multiple collisions, and the lifetime for dissociation. We derive absolute 0 and 298 K bond dissociation energies (BDEs) for all alkali metal ion−thiouracil complexes and compare these values to theoretical BDEs calculated here. Comparison is also made to literature values for analogous complexes of the alkali metal ions with uracil (U).[32] The trends in the measured and calculated BDEs are examined to determine the effects of the position and extent of thioketo or thioketo plus methyl substitution on the properties of uracil and its noncovalent interactions with alkali metal ions. Theoretical calculations are also performed to examine the influence of thioketo or thioketo plus methyl substitution on the dipole moments, polarizabilities, acidities, proton affinities, and Watson−Crick base pairing energies as well as implications for the stability of nucleic acids.

Experimental and Theoretical Section

Experimental Protocol. Cross sections for CID of M^+(SU), where $M^+ = Li^+$, Na^+, and K^+ and SU = 2SU, 5Me2SU, 6Me2SU, 4SU, and 24SU, are measured using guided ion beam mass spectrometers that have been described in detail previously.[40,41] The alkali metal ion−thiouracil complexes are formed by condensation of the alkali metal ion and neutral thiouracil in a flow tube ion source operating at a pressure in the range from 0.5 to 0.7 Torr. The complexes are collisionally stabilized and thermalized to room temperature by in excess of 10^5 collisions with the He and Ar bath gases such that ions emanating from the source are well described by a 298 K Maxwell−Boltzmann internal energy distribution. The ions are effusively sampled, focused, accelerated, and focused into a magnetic sector momentum analyzer for reactant ion selection. Mass-selected ions are decelerated to a desired kinetic energy and focused into an octopole ion guide. The octopole passes through a static gas cell containing Xe[42−44] at sufficiently low pressure, 0.04−0.20 mTorr, that multiple ion−neutral collisions are improbable. The octopole ion guide acts as an efficient radial trap[45] for ions such that scattered reactant and product ions are not lost as they drift toward the end of the octopole. These ions are focused into a quadrupole mass filter for mass analysis and subsequently detected with a secondary electron scintillation detector and standard pulse counting techniques.

In the present work, experiments for the Na^+(SU) and K^+(SU) complexes were carried out in an instrument that employs a 880 kHz resonator for the quadrupole mass filter (QMF). However, this set up exhibits significant mass discrimination for detection of low *m*/*z* product ions such as Li^+. Therefore, the Li^+(SU) complexes were studied in another GIBMS instrument[41] that uses a 1.2 MHz resonator for the QMF to improve the detection efficiency of Li^+. It has previously been show that this QMF oscillator does not suffer from the same low mass discrimination encountered with the 880 kHz resonator.[46]

Data Handling. Measured ion intensities are converted to absolute CID cross sections using a Beer's law analysis as described previously.[47] Errors in the pressure measurement and uncertainties in the length of the interaction region lead to ±20% uncertainties in the cross-section magnitudes, while relative uncertainties are approximately ±5%.

Ion kinetic energies in the laboratory frame, E_{lab}, are converted to energies in the center-of-mass (CM) frame, E_{CM}. All energies reported below are in the CM frame unless otherwise noted. The absolute zero and distribution of the ion kinetic energies are determined using the octopole ion guide as a retarding potential analyzer, as previously described.[47] The distribution of ion kinetic energies is nearly Gaussian with a fwhm in the range from 0.2 to 0.5 eV (lab) for these experiments. The uncertainty in the absolute energy scale is ±0.05 eV (lab).

Because multiple ion−neutral collisions can influence the shape of CID cross sections and the threshold regions are most sensitive to these effects, each CID cross section was measured twice at three nominal Xe pressures (0.05, 0.10, and 0.20 mTorr). Data free from pressure effects are obtained by extrapolating to zero pressure of the Xe reactant, as described previously.[42,48] Results reported below are due to single bimolecular encounters.

Theoretical Calculations. Stable structures, vibrational frequencies, and energetics for the neutral, deprotonated, protonated, and alkali metal ion−thiouracil complexes, as well as the Watson−Crick base pairs between adenine and uracil (A::U) and between adenine and the thiouracils (A::SU), and Na^+-

bound A::SU base pairs, were obtained from theoretical electronic structure calculations using Gaussian 98.[49] Geometry optimizations and vibrational analyses were performed at the MP2(full)/6-31G* level for all systems except the A::U and A::SU base pairs and the Na^+(A::SU) base pair complexes, where the larger size of these systems required use of the B3LYP/6-31G* level of theory. When used to model the data or calculate thermal energy corrections, the MP2(full)/6-31G* and B3LYP/6-31G* vibrational frequencies are scaled by a factors 0.9646 and 0.9804, respectively.[50] The vibrational frequencies and rotational constants of the ground state M^+(SU) complexes and neutral SU nucleobases are listed in Tables 1S and 2S of the Supporting Information. Single point energy calculations were performed at the MP2(full)/6-311+G(2d,2p) level using the MP2(full)/6-31G* and B3LYP/6-31G* optimized geometries. Zero point energy (ZPE) and basis set superposition error (BSSE) corrections were included in determination of the BDEs.[51,52]

In the present work, we only considered binding to these thiouracils at the most favorable binding sites, the keto and thioketo groups: O2 (S2) and O4 (S4). Stable minima were found for all three alkali metal ions binding at both the O2 (S2) and O4 (S4) positions for all five thiouracils. Binding to N1, N3, or the π electrons was not considered because these sites have previously been shown to be much less favorable.[32]

To more clearly visualize the influence of thioketo and thioketo plus methyl substitution on the electronic properties of uracil, we also calculated electrostatic potential maps for the ground state geometries of uracil and the thiouracils. The process involves calculation of the interaction between a +1 probe charge and every part of the electron density cloud of these species. The electrostatic potential is then mapped onto an isosurface of the total SCF electron density (0.04 au for the maps generated in this work) of the species of interest. The electrostatic potential maps generated via this procedure are then color-coded according to their potential with the regions of greatest electrostatic potential shown in red and those with the least shown in blue.

Thermochemical Analysis. The threshold regions of the CID cross sections are modeled using eq 1

$$\sigma(E) = \sigma_0 \sum_i g_i (E + E_i - E_0)^n / E \qquad (1)$$

where σ_0 is an energy-independent scaling factor, E is the relative translational energy of the reactants, E_0 is the threshold for reaction of the ground electronic and ro-vibrational state, and n is an adjustable parameter that describes the efficiency of kinetic to internal energy transfer.[41] The summation is over the ro-vibrational states of the reactant ions, i, where E_i is the excitation energy of each state and g_i is the relative population of each state ($\Sigma g_i = 1$).

The Beyer−Swinehart algorithm[53] is used to evaluate the density of the ro-vibrational states, i, and the relative populations of those states, g_i, are calculated from the 298 K Maxwell−Boltzmann distribution appropriate for the reactants. Vibrational frequencies and rotational constants of the reactant complexes are determined as described in the Theoretical Calculations section and listed in the Supporting Information in Tables 1S and 2S, respectively. The average vibrational energies at 298 K of the thiouracils and alkali metal ion−thiouracil complexes are also given in Table 1S. We estimated the sensitivity of our analysis to the deviations from the true frequencies by scaling the calculated frequencies by ±10% as suggested by Pople et al.[54] The corresponding change in the average vibrational energy

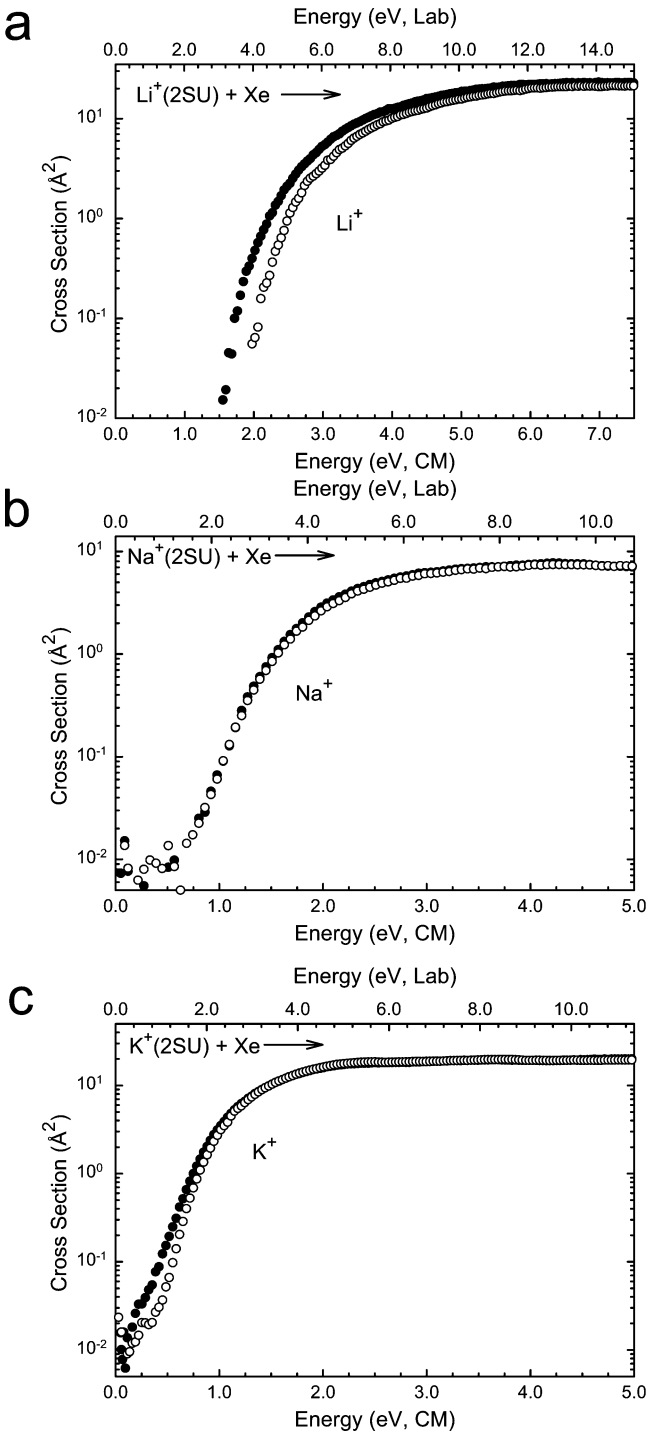

Figure 2. Cross sections for the collision-induced dissociation of M^+(2SU) complexes with Xe as a function of collision energy in the center-of-mass frame (lower *x*-axis) and laboratory frame (upper *x*-axis). Data for the M^+ product channel are shown for a Xe pressure of 0.2 mTorr (●) and extrapolated to zero (○).

is taken to be an estimate of one standard deviation of the uncertainty in vibrational energy (Table 1S) and is included in the uncertainties listed with the E_0 values.

As described in detail elsewhere,[39,55] statistical theories for unimolecular dissociation are included in eq 1 to account for the possibility that collisionally activated M^+(SU) complex ions do not dissociate on the time scale of our experiment ($\sim 10^{-4}$ s). This requires sets of ro-vibrational frequencies appropriate for the energized molecules and the transition states (TSs) leading to dissociation. The former are given in Tables 1S and

TABLE 1: Threshold Dissociation Energies at 0 K, and Entropies of Activation at 1000 K[a]

M^+L	σ_0[b]	n_b	E_0[c] (eV)	E_0(PSL) (eV)	kinetic shift (eV)	$\Delta S^\dagger$(PSL) (J mol^{-1} K^{-1})[d]
Li^+(2SU)	18.0 (1.0)	1.5 (0.1)	2.49 (0.05)	2.24 (0.06)	0.25	25 (2)
Na^+(2SU)	10.3 (0.3)	1.2 (0.1)	1.57 (0.03)	1.45 (0.04)	0.12	22 (2)
K^+(2SU)	28.8 (0.9)	1.2 (0.1)	1.10 (0.03)	1.07 (0.03)	0.03	19 (2)
Li^+(5Me2SU)	11.5 (0.3)	1.7 (0.1)	2.71 (0.03)	2.21 (0.06)	0.50	26 (2)
Na^+(5Me2SU)	3.9 (0.1)	1.0 (0.1)	1.70 (0.07)	1.47 (0.06)	0.23	25 (2)
K^+(5Me2SU)	5.4 (0.9)	1.3 (0.1)	1.12 (0.04)	1.05 (0.03)	0.07	21 (2)
Li^+(6Me2SU)	12.1 (1.0)	1.7 (0.1)	2.87 (0.05)	2.30 (0.06)	0.57	25 (2)
Na^+(6Me2SU)	11.1 (0.4)	1.3 (0.1)	1.73 (0.03)	1.49 (0.04)	0.24	23 (2)
Na^+(6Me2SU)	32.4 (1.9)	1.0 (0.1)	1.19 (0.05)	1.02 (0.04)	0.17	21 (2)
Li^+(4SU)	9.1 (0.5)	1.7 (0.1)	2.50 (0.04)	2.21 (0.05)	0.29	24 (2)
Na^+(4SU)	13.7 (1.0)	1.4 (0.1)	1.38 (0.06)	1.30 (0.05)	0.08	22 (2)
K^+(4SU)	31.9 (2.6)	1.1 (0.1)	1.03 (0.08)	1.01 (0.06)	0.02	17 (2)
Li^+(24SU)	11.4 (0.8)	1.6 (0.1)	2.00 (0.04)	1.82 (0.05)	0.18	20 (2)
Na^+(24SU)	2.2 (1.4)	1.7 (0.3)	1.07 (0.07)	1.04 (0.06)	0.03	19 (2)
K^+(24SU)	42.6 (1.7)	1.0 (0.1)	0.86 (0.03)	0.84 (0.03)	0.02	3 (2)

[a] Uncertainties are listed in parentheses. [b] Average values for loose PSL transition state. [c] No RRKM analysis. [d] Difference between E_0 and E_0(PSL).

2S, while we assume that the TSs are loose and product-like because the interaction between the alkali metal ion and thiouracil is largely electrostatic, a treatment that corresponds to a phase space limit (PSL), as described in detail elsewhere.[39] In the present work the adiabatic 2-D rotational energy is treated using a statistical distribution with explicit summation over the possible values of the rotational quantum number.[39]

The model represented by eq 1 is appropriate for translationally driven reactions[56] and has been found to reproduce CID cross sections well. The model is convoluted with the kinetic and internal energy distributions of both reactants, and a nonlinear least-squares analysis of the data is performed to give optimized values for the parameters σ_0, E_0, and n. The error associated with the measurement of E_0 is estimated from the range of threshold values determined for eight zero-pressure-extrapolated data sets, variations associated with uncertainties in the vibrational frequencies, and the error in the absolute energy scale, 0.05 eV (lab). For analyses that include the RRKM lifetime effect, the uncertainties in the reported E_0(PSL) values also include the effects of increasing and decreasing the time assumed available for dissociation by a factor of 2.

Equation 1 explicitly includes the internal energy of the ion, E_i. All energy available is treated statistically because the internal energy of the reactants is redistributed throughout the M^+(SU) complex upon collision with the Xe atom. Because the CID processes examined here are simple noncovalent bond fission reactions, the E_0(PSL) values determined by analysis with eq 1 can be equated to 0 K BDEs.[57,58]

Results

Cross Sections for Collision-Induced Dissociation. Experimental cross sections were obtained for the interaction of Xe with 15 M^+(SU) complexes, where $M^+ = Li^+$, Na^+, and K^+ and SU = 2SU, 4SU, 24SU, 5Me2SU, and 6Me2SU. Figure 2 shows representative data for the M^+(2SU) complexes. All other M^+(SU) complexes exhibit similar behavior, and analogous results for these systems are shown in Figure 1S in the Supporting Information. The dominant process for all complexes is loss of the intact neutral thiouracil in the CID reactions 2.

$$M^+(SU) + Xe \rightarrow M^+ + SU + Xe \qquad (2)$$

The magnitudes of the CID cross sections generally increase in size from Li^+ to Na^+ to K^+, largely because the thresholds decrease in this same order. In several systems ligand-exchange processes to form M^+Xe are also observed as minor reaction pathways, eq 3

$$M^+(SU) + Xe \rightarrow M^+Xe + SU \qquad (3)$$

The cross sections for these products are more than 2 orders of magnitude smaller than those for the primary M^+ product. It is likely that such ligand-exchange processes occur for all complexes but that the signal-to-noise in the other experiments was not sufficient to differentiate the M^+Xe product from background noise. These M^+Xe cross sections will not be discussed further as little systematic information can be extracted from these products.

Threshold Analyses. The model of eq 1 was used to analyze the thresholds for reactions 2 in 15 M^+(SU) systems. The results of these analyses are provided in Table 1, and representative results are shown in Figure 3 for the M^+(2SU) complexes. Results for all other complexes are shown in Figure 2S of the Supporting Information. In all cases the experimental CID cross sections for reactions 2 are accurately reproduced using a loose PSL TS model.[39] Previous work has shown that this model provides the most accurate assessment of the kinetic shifts for CID processes for electrostatic ion−molecule complexes. Good reproduction of the data is obtained over energy ranges exceeding 2 eV and cross-section magnitudes of at least a factor of 100. Table 1 also includes values of E_0 obtained without including the RRKM lifetime analysis. Comparison of these values with the E_0 (PSL) values shows that the kinetic shifts vary with the strength of the alkali metal ion−thiouracil interaction such that the kinetic shifts are smallest for the K^+ complexes, increase for the Na^+ complexes, and are largest for the Li^+ complexes. This trend is expected because the kinetic shift is correlated to the density of states of the activated complex at the threshold, which increases with energy.

The entropy of activation, $\Delta S^\dagger$, is a measure of the looseness of the TS and also a reflection of the complexity of the system. It is largely determined by the molecular parameters used to model the energized molecule and the TS but also depends on the threshold energy. The $\Delta S^\dagger$(PSL) values at 1000 K are listed in Table 1 and vary between 3 and 26 J/K mol across these systems. The values are largest for the Li^+(SU) complexes and decrease with increasing size of the alkali metal ion in accord with the threshold energies for these systems.

Theoretical Results. Theoretical structures for the neutral, deprotonated, protonated, and alkali metalated SU nucleobases,

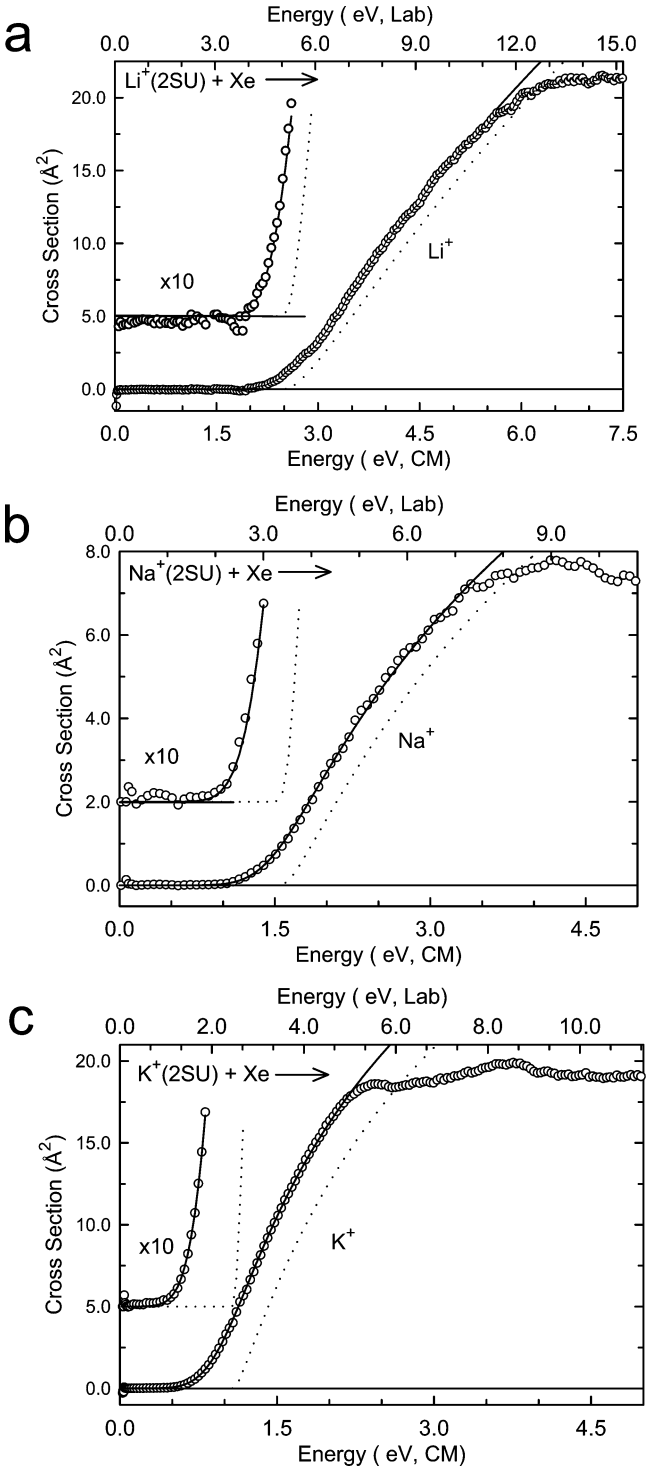

Figure 3. Zero-pressure-extrapolated cross sections for collision-induced dissociation of the M^+(2SU) complexes with Xe in the threshold region as a function of kinetic energy in the center-of-mass frame (lower *x*-axis) and laboratory frame (upper *x*-axis). The solid lines show the best fits to the data using eq 1 convoluted over the neutral and ion kinetic-energy distributions. The dashed lines show the model cross sections in the absence of experimental kinetic-energy broadening for reactants with an internal energy corresponding to 0 K.

as well as the A::U and A::SU Watson−Crick base pairs, were calculated as described in the Theoretical Calculations section. Details of the optimized geometries for the ground state conformations of the neutral SU nucleobases, M^+(SU) complexes, and A::U and A::SU Watson−Crick base pairs are provided in the Supporting Information, Table 3S. Results for the most stable conformations of the Na^+(SU) complexes are

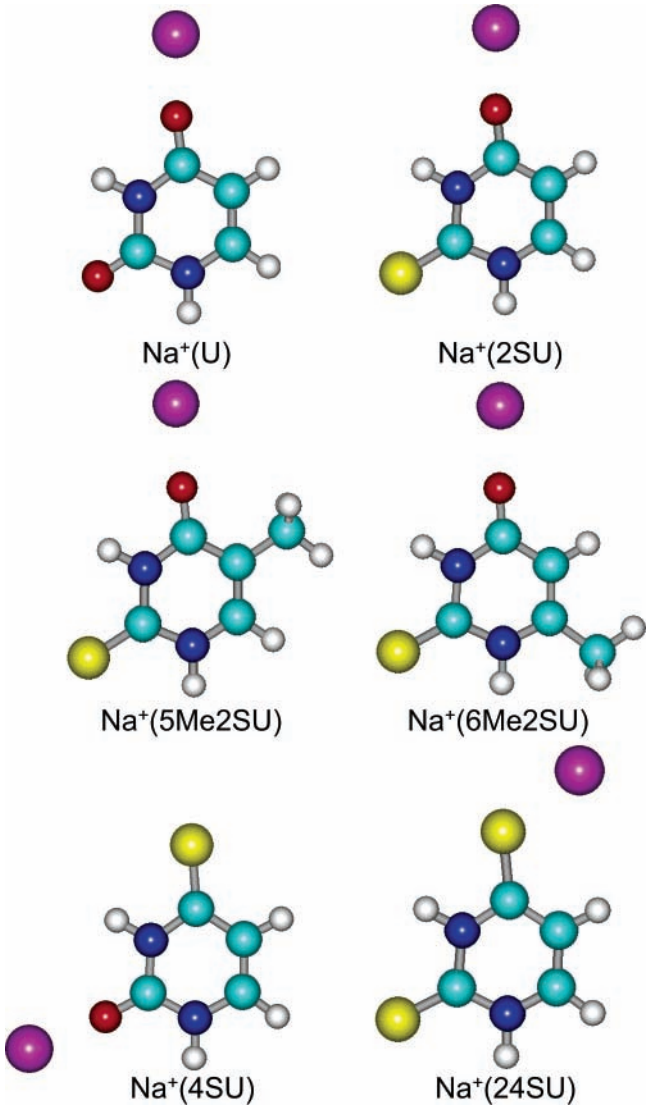

Figure 4. MP2(full)/6-31G* optimized geometries of Na^+(U) and Na^+(SU), where SU = 2SU, 5Me2SU, 6Me2SU, 4SU, and 24SU.

shown in Figure 4 for each thiouracil.[59] Structures for the Li^+(SU) and K^+(SU) complexes are very similar to those for Na^+(SU) except for the M^+−SU bond distance. The 0 K calculated proton and alkali metal ion binding energies are listed in Table 2. Independent ZPE and BSSE corrections are made for all conformers listed. Geometrical parameters of the ground state-optimized structures of the neutral, protonated, and alkali-metalated SU nucleobases are summarized in Table 3. The electrostatic potential maps of uracil and the thiouracils are shown in Figure 5. The 0 K calculated acidities of the SU nucleobases are listed in Table 4. The 0 K calculated base pairing energies of the A::SU and Na^+(A::SU) Watson−Crick base pair complexes are listed in Table 5. The optimized structures of the A::SU base pairs are shown in Figure 6, while those for Na^+(A::SU) base pair complexes are shown in Figure 7 and Figure 3S of the Supporting Information.

Electronic Properties. Thioketo substitution of uracil alters its electronic properties (e.g., dipole moments, polarizabilities, and electrostatic potential), which in turn alter the acidity, proton affinity, and alkali metal ion binding affinities of uracil. Thus, it is useful to examine changes in these electronic properties of uracil upon thioketo substitution in order to understand how these changes might alter the reactivity and stability of uracil and nucleic acids. The calculated dipole moments and estimated

TABLE 2: Calculated and Experimental Enthalpies of Proton and Alkali Metal Ion Binding to Uracil and Thiouracils at 0 K in kJ/mol

	experiment		theory		
complex	TCID[a]	binding site	D_e[b]	D_0[c]	$D_{0,BSSE}$[d]
H^+(U)	866.6[e]	O4	879.5	846.7	837.5
	868 (13)[f]		867.6	835.5	826.4
	835 (13)[f]	O2	845.2	815.1	805.8
			840.2	810.4	801.0
Li^+(U)[g]	211.5 (6.1)	O4	207.5	201.2	194.9
		O2	192.0	186.7	180.5
		π	68.3	65.0	56.5
Na^+(U)[g]	134.6 (3.4)	O4	146.2	142.5	134.5
		O2	132.6	129.7	122.8
K^+(U)[g]	104.3 (2.8)	O4	110.8	107.8	103.8
		O2	98.4	96.1	92.2
H^+(2SU)	879.5 (8.8)[h]	O4	879.5	846.9	837.6
			867.8	836.4	827.2
		S2	862.2	839.2	826.7
			860.2	837.3	824.6
Li^+(2SU)	216.2 (5.7)	O4	205.0	199.2	192.8
		S2	149.4	145.1	138.5
Na^+(2SU)	139.8 (3.3)	O4	143.5	140.2	133.1
		S2	102.8	100.3	94.2
K^+(2SU)	103.2 (2.6)	O4	108.1	105.5	101.4
		S2	72.2	70.6	67.4
H^+(5Me2SU)		O4	885.1	853.5	844.0
			874.4	843.1	834.0
		S2	876.5	853.6	841.0
			874.5	851.8	839.2
Li^+(5Me2SU)	213.3 (5.5)	O4	205.0	199.4	193.0
		S2	158.9	154.8	148.3
Na^+(5Me2SU)	142.3 (5.5)	O4	142.7	139.5	132.2
		S2	110.8	108.4	102.4
K^+(5Me2SU)	101.2 (2.8)	O4	107.2	104.7	100.5
		S2	78.8	77.4	74.2
H^+(6Me2SU)		O4	895.7	864.5	855.2
			884.2	853.6	844.5
		S2	874.2	851.5	839.1
			872.1	849.9	836.8
Li^+(6Me2SU)	222.0 (6.2)	O4	214.0	208.5	202.1
		S2	157.2	153.1	146.6
Na^+(6Me2SU)	143.6 (3.8)	O4	150.6	147.6	140.5
		S2	109.5	107.1	101.1
K^+(6Me2SU)	106.6 (3.5)	O4	114.2	111.9	107.8
		S2	77.8	76.4	73.2
H^+(4SU)	882.8 (8.8)[h]	S4	888.9	862.0	852.1
			886.9	863.9	850.3
		O2	846.9	817.2	807.9
			842.6	813.4	804.0
Li^+(4SU)	213.1 (5.0)	O2	191.5	186.6	180.1
		S4	158.6	153.8	147.3
			153.7	148.8	142.3
Na^+(4SU)	125.8 (4.7)	O2	131.8	129.2	122.1
		S4	109.7	107.3	101.3
			106.7	103.6	97.6
K^+(4SU)	97.3 (5.5)	O2	97.2	95.8	91.7
		S4	77.4	75.5	72.3
			76.0	73.9	70.9
H^+(24SU)	886.6 (11.7)[h]	S4	888.4	863.6	851.7
			886.6	861.7	850.0
		S2	863.7	840.3	827.7
			862.0	838.7	825.9
Li^+(24SU)	175.1 (4.5)	S4	156.5	151.6	144.9
			152.4	147.3	140.6
		S2	149.6	145.0	138.2
Na^+(24SU)	100.2 (5.8)	S4	107.7	104.6	98.4
			105.3	102.2	95.8
		S2	102.7	99.8	93.5
K^+(24SU)	80.8 (2.8)	S4	75.0	72.8	69.7
			74.5	72.1	69.0
		S2	71.9	69.9	66.6

[a] Threshold collision-induced dissociation except as noted. [b] Calculated at the MP2(full)/6-311+G(2d,2p) level of theory using MP2(full)/6-31G* optimized geometries. [c] Including ZPE corrrections with frequencies scaled by 0.9646. [d] Also includes BSSE corrections. [e] Ref 61. [f] Ref 64. [g] Ref 32. [h] Ref 63.

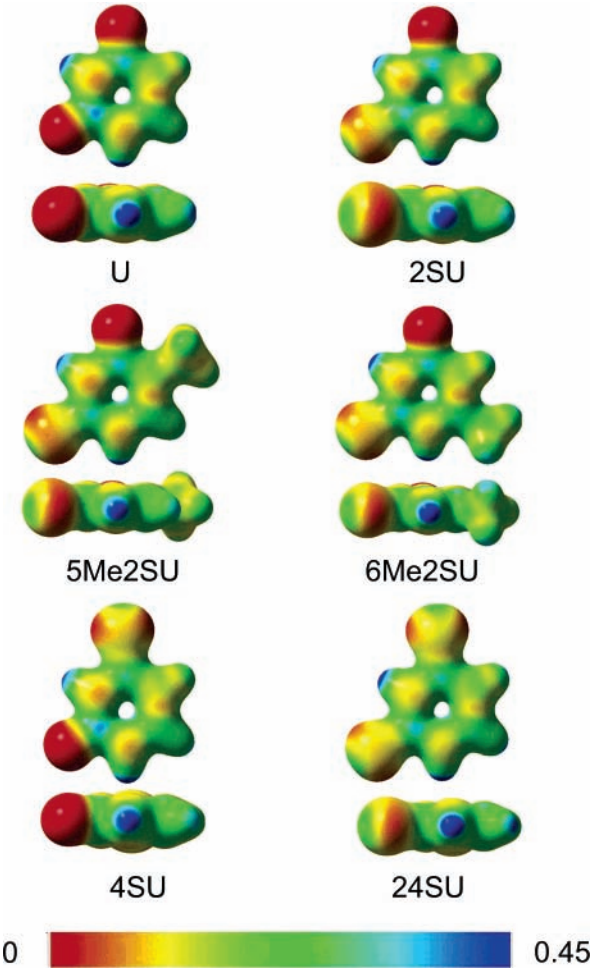

Figure 5. Electrostatic potential maps of uracil and the thiouracils at an isosurface of 0.04 au of the total SCF electron density.

polarizabilities[38] of uracil and the thiouracils are summarized in Figure 1. In all cases, the center-of-mass and electron density distribution of uracil is altered upon thioketo or thioketo and methyl substitution, thereby enhancing both the dipole moment and the polarizability of uracil. Thioketo substitution of uracil at the 4-position leads to a larger increase in the dipole moment than does substitution at the 2-position. Similarly, methylation at the 6-position produces a larger increase in the dipole moment than when substitution occurs at the 5-position. In contrast, enhancement in the polarizability varies with the nature of the substituent and extent of substitution but is insensitive to the position(s) of substitution. Thioketo substitution results in a larger increase in the polarizability than does methylation. The estimated polarizability increases upon thioketo substitution from 9.69Å^3 for U to 12.68 Å^3 for 2SU and 4SU and to 15.77 Å^3 for 24SU. Similarly, the polarizability increases upon methylation from 12.68 Å^3 for 2SU to 15.50 Å^3 for 5Me2SU and 6Me2SU. In the absence of other effects enhancements in the dipole moments and polarizabilities of the thiouracils relative to uracil should result in stronger binding in the M^+(SU) complexes as compared to the corresponding M^+(U) complex.

The electrostatic potential maps of uracil and the thiouracils were calculated as described in the Theoretical Calculations section and are shown in Figure 5. As can be seen in the figure, the regions of greatest electron density in uracil occur at the keto oxygen atoms, O2 and O4, while significant electron density also exists at N1, N3, and between the C5 and C6 atoms. The electron density about the keto oxygen atoms is fairly isotropic. Thioketo substitution significantly alters the local

TABLE 3: Geometrical Parameters of MP2(full)/6-31G* Geometry Optimized Structures of Protonated and Alkali Metalated Uracil and Thiouracils

	X4 bonding					X2 bonding				
	bond length (Å)			bond angle (deg)		bond length (Å)			bond angle (deg)	
species	C4═X	M^+−X	N3−H	∠C4XM^+	∠N3C4XM^+	C2═X	M^+−X	N3−H	∠C2XM^+	∠N1C2XM^+
U[a]	1.226		1.017			1.223		1.017		
H^+(U)[a]	1.310	0.970	1.020	112.4	180.0	1.316	0.970	1.020	114.1	180.0
	1.310	0.980	1.020	114.8	0.1	1.310	0.097	1.020	114.7	0.5
Li^+(U)[a]	1.263	1.750	1.019	171.9	180.0	1.262	1.755	1.018	173.4	180.0
Na^+(U)[a]	1.255	2.109	1.019	173.2	180.0	1.253	2.116	1.018	173.0	180.0
K^+(U)[a]	1.249	2.482	1.018	174.7	180.0	1.247	2.493	1.018	173.1	180.0
2SU	1.220		1.018			1.648		1.018		
H^+(2SU)	1.310	0.970	1.020	112.3	180.0	1.730	1.341	1.020	95.5	±156.8
	1.315	0.980	1.020	114.8	0.0	1.730	1.341	1.020	95.8	±27.4
Li^+(2SU)	1.255	1.740	1.010	172.3	180.0	1.705	2.310	1.010	109.5	± 58.9
Na^+(2SU)	1.255	2.100	1.010	174.0	180.0	1.693	2.658	1.010	113.7	±52.3
K^+(2SU)	1.249	2.480	1.019	175.6	180.0	1.678	3.097	1.010	134.4	±35.6
5Me2SU	1.220		1.010			1.650		1.010		
H^+(5Me2SU)	1.310	0.970	1.020	117.8	180.0	1.740	1.340	1.020	94.9	±149.3
	1.319	0.980	1.020	114.6	0.0	1.740	1.340	1.020	95.0	±32.8
Li^+(5Me2SU)	1.260	1.746	1.020	175.8	178.7	1.708	2.300	1.010	109.0	±57.2
Na^+(5Me2SU)	1.250	2.100	1.010	177.3	179.9	1.696	2.651	1.010	113.2	±54.0
K^+(5Me2SU)	1.252	2.483	1.010	177.3	178.0	1.682	3.080	1.010	133.3	±41.6
6Me2SU	1.227		1.010			1.650		1.010		
H^+(6Me2SU)	1.310	0.979	1.020	112.0	180.0	1.742	1.340	1.020	95.1	±155.9
	1.310	0.970	1.020	114.5	0.0	1.742	1.340	1.020	95.1	±28.6
Li^+(6Me2SU)	1.260	1.740	1.010	172.6	178.7	1.707	2.307	1.010	109.0	±54.4
Na^+(6Me2SU)	1.250	2.100	1.010	174.0	177.8	1.690	2.653	1.010	113.0	±51.2
K^+(6Me2SU)	1.250	2.477	1.010	176.2	178.0	1.681	3.091	1.010	133.6	±33.5
4SU	1.645		1.010			1.222		1.010		
H^+(4SU)	1.724	1.340	1.020	95.3	180.0	1.317	0.970	1.020	114.6	0.0
	1.720	1.340	1.020	96.9	0.0	1.310	0.970	1.020	114.1	180.0
Li^+(4SU)	1.690	2.306	1.020	110.7	±146.8	1.263	1.750	1.020	173.8	180.0
	1.696	2.300	1.020	112.9	±52.8					
Na^+(4SU)	1.680	2.657	1.020	116.2	±146.7	1.254	2.110	1.010	173.2	180.0
	1.684	2.650	1.010	118.0	±49.4					
K^+(4SU)	1.670	3.070	1.020	138.2	180.0	1.249	2.490	1.010	173.0	180.0
	1.660	3.070	1.020	145.4	0.0					
24SU	1.646		1.010			1.222		1.010		
H^+(24SU)	1.726	1.340	1.020	95.2	180.0	1.740	1.340	1.020	94.9	±34.3
	1.720	1.340	1.020	96.9	0.0	1.742	1.340	1.020	95.0	±151.8
Li^+(24SU)	1.690	2.306	1.020	110.3	±144.5	1.700	2.311	1.020	109.1	±56.3
	1.690	2.300	1.020	112.6	±53.1					
Na^+(24SU)	1.680	2.651	1.020	115.6	±145.2	1.254	2.659	1.010	113.2	±52.6
	1.680	2.650	1.010	117.8	±48.2					
K^+(24SU)	1.671	3.070	1.020	139.1	180.0	1.249	3.104	1.010	133.4	±36.7
	1.660	3.080	1.010	145.3	0.0					

[a] Reference 32.

electrostatic potential but only minimally impacts the electrostatic potential of the remainder of the molecule. Clearly, the sulfur atom is larger than the oxygen atom. This leads to the electron density being distributed over a greater volume. Sulfur is also less electronegative than oxygen, and therefore, less electron density is localized around the sulfur nuclei. In addition, the electron density around the sulfur nuclei is not nearly as isotropic as it is around the oxygen nuclei and is slightly less isotropic for thioketo substitution at the 4-position than at the 2-position. In either case, the electron density is greatest on the sides of the sulfur atom, indicating sp^2 hybridization. Thus, both the strength and the geometry of noncovalent binding of protons or metal ions to uracil as well as hydrogen bonding interactions with uracil are likely to be altered upon thioketo substitution. The effects of methylation on the electrostatic potential are less significant in terms of its influence on the binding of protons or metal ions or hydrogen bonding interactions with uracil, primarily because the methyl group is not directly involved in the binding. Clearly, the methyl group is much larger than the hydrogen atom. However, the methyl group does not interfere with binding at the O2 (S2) or O4 (S4) position. 5-Methylation leads to a slight increase whereas 6-methylation leads to a decrease in the electron density at S2. More importantly, methylation at either position does not noticeably affect the electron density at O4. Thus, the strength and geometry of noncovalent binding of protons or metal ions to uracil as well as hydrogen bonding interactions with uracil are unlikely to be significantly influenced upon methylation at these sites.

Alkali Metal Ion Binding. The optimized structures obtained for the isolated SU nucleobases and the M^+(SU) complexes are summarized in Tables 3 and 3S. Changes in the structure of uracil and the thiouracils upon alkali metal ion complexation are minor (Table 3). Similar to that found for uracil,[32] the calculations find that the preferred binding site for all three alkali metal ions to 2SU, 5Me2SU, and 6Me2SU is at the O4 position. In all cases 2-thioketo substitution has very little effect on the O4 binding affinities and results in a small decrease (∼3 kJ/mol) as compared to U, 5MeU, and 6MeU.[32,34] The C═O−M^+ bond angle is very nearly linear but shifted slightly *away* from the adjacent N3H group and the direction of the global dipole moment, Figure 1. Apart from the methyl hydrogen atoms, all of these complexes are planar. In previous work on

TABLE 4: Calculated Enthalpies of Deprotonation of Uracil and Thiouracils at 0 K in kJ/mol[a]

species	deprotonation site	theory (MP2(full)) D_e	theory (MP2(full)) D_0[b]	theory (MP2(full)) $D_{0,BSSE}$[c]	literature experiment[d]	literature theory[e]	literature CBS-Q[f]
U	N1	1422.5	1387.0	1377.0	1393 (17) 1393 (21)[h]	1391.0[g] 1377[d] 1400[h] 1398[i]	1390.7
2SU	N1	1394.1	1360.3	1350.0		1364.2[g]	
5Me2SU	N1	1399.8	1365.7	1355.3			
6Me2SU	N1	1399.8	1365.6	1355.1			
4SU	N1	1388.5	1354.8	1344.9		1359.6[g]	
24SU	N1	1366.6	1333.7	1323.5		1338.8[g]	
U	N3	1475.3	1436.5	1426.4	1452 (17)	1447.1[g] 1433[d] 1450[h] 1450[i]	1440.7
2SU	N3	1441.0	1404.9	1394.6		1401.0[g]	
5Me2SU	N3	1443.6	1407.7	1397.3			
6Me2SU	N3	1447.1	1411.1	1400.8			
4SU	N3	1447.3	1411.0	1400.6		1418.2[g]	
24SU	N3	1421.5	1386.4	1375.7		1392.4[g]	

[a] MP2(full)/6-311+G(2d,2p)//MP2(full)/6-31G*. [b] Includes ZPE corrections. [c] Also includes BSSE corrections. [d] Ion−molecule reaction bracketing. Reference 68. [e] Calculated at the B3LYP/6-31+G(d,p) level of theory, expect as noted. [f] Reference 34. [g] Reference 62. [h] Reference 69. Ion−molecule reaction bracketing, calculated at the G3 level of theory. [i] Reference 71. Calculated at the B3LYP/aug-cc-pVTZ//B3LYP/6-31G(d) level of theory.

TABLE 5: Calculated Hydrogen Bond Lengths (Å) and Enthalpies (kJ/mol) of Base Pairing of A::U, A::(SU), Na^+(A::U), and Na^+(A::SU) at 0 K[a]

species	hydrogen-bond lengths N···HN	hydrogen-bond lengths NH···O (S)	enthalpies (MP2(full)) D_e	enthalpies (MP2(full)) D_0[b]	enthalpies (MP2(full)) $D_{0,BSSE}$[c]
A::U[d]	1.830	1.929	69.9	63.9	51.0
A::2SU	1.896	1.895	71.3	65.6	51.2
A::4SU	1.902	2.462	65.4	60.6	47.0
A::5Me2SU	1.897	1.897	71.3	65.5	51.3
A::6Me2SU	1.897	1.890	71.0	65.4	50.9
A::24SU	2.075	2.393	58.5	54.0	40.3
Na^+N_3(A::U)[d]	1.831	1.927	88.0	82.1	68.4
Na^+N_3(A::2SU)	1.878	1.915	95.7	90.1	74.8
Na^+N_3(A::4SU)	1.884	2.626	92.4	88.1	72.4
Na^+N_3(A::24SU)	2.023	2.751	90.2	86.3	70.2
Na^+(N7/NH_2(A::U)[d]	1.950	1.815	86.6	81.2	68.0
Na^+(N7/NH_2(A::2SU)	1.998	1.820	87.8	84.6	70.7
Na^+(N7/NH_2(A::4SU)	1.972	2.377	82.8	80.3	66.4
Na^+(N7/NH_2(A::24SU)	2.105	2.332	80.6	78.6	64.2
Na^+O_2(A::U)[d]	1.894	2.240	124.9	117.5	99.9
Na^+S_2(A::2SU)	1.984	2.034	138.1	111.1	91.6
Na^+O_2(A::4SU)	1.973	2.794	123.1	117.9	100.4
Na^+S_2(A::24SU)	1.975	2.566	128.5	123.8	104.4
Na^+O_4(A::U)[d]	1.986		114.4	105.8	91.4
Na^+O_4(A::2SU)	2.055		114.9	108.6	93.7
Na^+S_4(A::4SU)	2.161		135.3	128.8	112.6
Na^+S_4(A::24SU)	2.283		135.3	129.8	111.6

[a] MP2(full)/6-311+G(2d,2p)//B3LYP/6-31G*. [b] Includes ZPE corrections. corrections. [c] Also includes BSSE. [d] Reference 34.

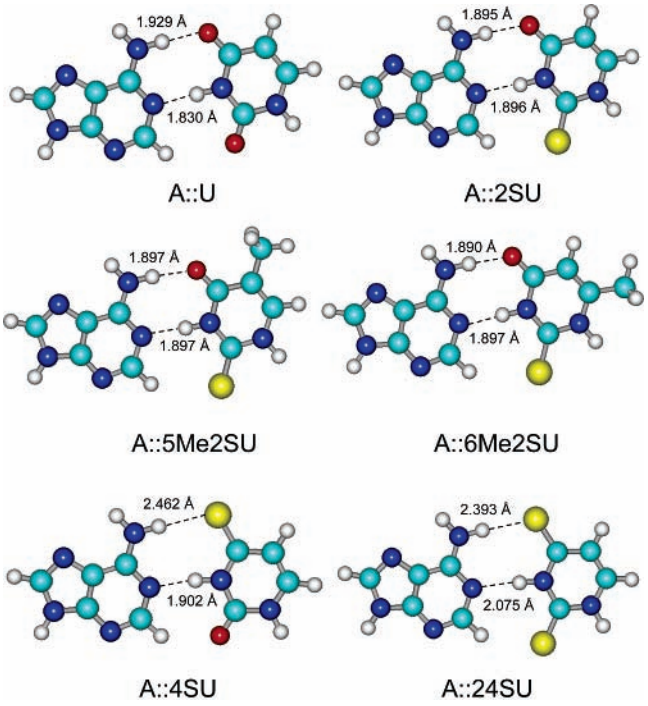

Figure 6. B3LYP/6-31G* optimized geometries of A::U and A::SU base pairs, where SU = 2SU, 5Me2SU, 6Me2SU, 4SU, and 24SU.[40]

uracil the O2 binding site was found to be less favorable than O4 by 14.4, 11.7, and 11.6 kJ/mol for Li^+, Na^+, and K^+, respectively.[32] In contrast, the calculations find two equivalent and significantly less favorable binding sites at S2. The C═S−M^+ bond angle varies from approximately 109° to 135° as the metal ion changes from Li^+ to K^+ with the metal ion directed toward the adjacent N3H group. In addition, the complexes are no longer planar. The N−C═S−M^+ dihedral angle varies from approximately ±59° to ±34° as the metal ion changes from Li^+ to K^+. The electrostatic potential maps of 2SU, 5Me2SU, and 6Me2SU suggest that binding in the plane would be more favorable as the electrostatic potential is greatest near the plane of the molecule. However, repulsive interactions with the H atom on the adjacent N3 atom make it more favorable for the metal ion to bind out of the plane of the molecule. The dihedral angle decreases as the size of the alkali metal ion increases because the distance between the alkali metal ion and the hydrogen atom is longer and therefore experiences reduced steric repulsion. The dihedral angles are slightly larger for 5Me2SU than 2SU and 6Me2SU because the 5-methyl substituent leads to greater electron density out of the plane near S2. Analogous starting structures in which the alkali metal ion binds at S2 but is directed toward the N1H group always converged to one of the two above structures in which the alkali metal ion is directed toward the N3H group. The larger size of the sulfur atom and therefore longer M^+−S2 bond (Table 3) as well as the decreased electrostatic potential around the sulfur atom make the S2

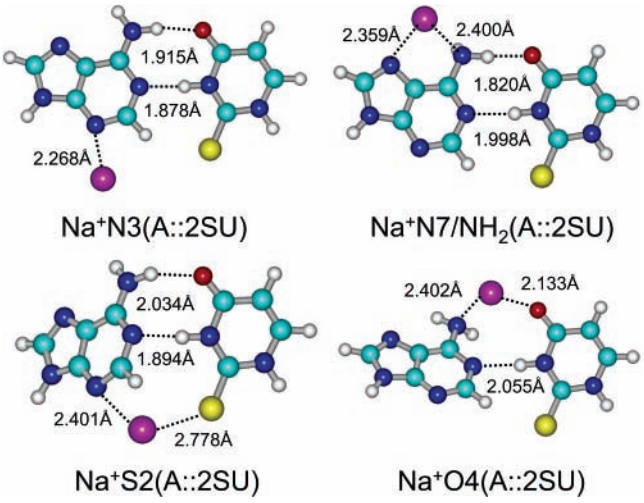

Figure 7. B3LYP/6-31G* optimized geometries of Na^+X(A::2SU) base pairs, where X = N3, N7/NH2, S2, and O4.

binding sites of 2SU less favorable than O4 by 54.3, 36.9, and 34.0 kJ/mol for Li^+, Na^+, and K^+, respectively. Similar results are found for 5Me2SU and 6Me2SU. However, the differences in the O4 and S2 binding affinities of 5Me2SU are smaller because the methyl group enhances the binding affinity at S2 more than it does at O4, as expected based upon the electrostatic potential maps (Figure 5).

In contrast to that found for U,[32] 2SU, 5Me2SU, and 6Me2SU, the preferred binding site for all three alkali metal ions to 4SU is at the O2 position. In all cases 4-thioketo substitution has very little effect on the O2 binding affinities and results in a small decrease (<1 kJ/mol) as compared to U.[32] This change in the preferred binding site clearly establishes that oxygen is a better donor than sulfur. The C═O−M^+ bond angle is again very nearly linear and shifted slightly *toward* the adjacent N3H group and the direction of the global dipole moment, Figure 1. All of these complexes are planar. In contrast, the calculations find four, two equivalent pairs, considerably less favorable binding sites at S4 for Li^+ and Na^+, while only two, an equivalent pair, considerably less favorable binding sites at S4 are found for K^+. The C═S−M^+ bond angle varies from ∼110° to 140° as the alkali metal ion varies from Li^+ to K^+, where the structures with the metal ion directed toward the adjacent C5H group are slightly more energetically favorable than those directed toward the adjacent N3H group. The complexes to Li^+ and Na^+ are nonplanar, whereas the K^+ complexes are essentially planar. The N−C═S−M^+ dihedral angle varies from approximately ±53° to ±49° to 0° as the alkali metal ion changes from Li^+ to Na^+ to K^+. The dihedral angle decreases as the size of the alkali metal ion increases because the alkali metal ion is further from the adjacent hydrogen atom and therefore experiences reduced steric repulsion. Again, the electrostatic potential map of 4SU suggests that binding in the plane would be more favorable. However, repulsive interactions with the hydrogen atom on the adjacent C5 (or N3) atom make it more favorable for the alkali metal ion to bind out of the plane of the molecule for Li^+ and Na^+, whereas K^+ is far enough from the hydrogen atom that it is able to bind in plane. Again, the larger size of the sulfur atom and therefore longer M^+−S4 bond (Table 3) as well as the decreased electrostatic potential around the sulfur atom make the S4 binding sites of 4SU less favorable than O2 by 32.8, 20.8, and 19.4 kJ/mol for Li^+, Na^+, and K^+, respectively. Compared to the O4 site of U, binding at S4 is less favorable by 47.6, 33.2, and 31.5 kJ/mol for Li^+, Na^+, and K^+, respectively, clearly indicating that oxygen binding is favored over binding to sulfur.

In contrast to that found for uracil and all of the other thiouracils examined here, the preferred binding site for all three alkali metal ions to 24SU is at the S4 position. The lack of oxygen binding sites reestablishes the 4-position as the most favorable for cation binding. In all cases 2,4-dithioketo substitution results in a significant decrease in the alkali metal ion binding affinities as compared to uracil and all of the other thiouracils examined here, primarily because no oxygen donor is available. This decrease in the binding affinities again clearly establishes that oxygen is a better donor than sulfur. As might be expected, the binding of alkali metal ions to 24SU parallels that found for S4 binding to 4SU and S2 binding to 2SU both in terms of the number and geometry of the stable conformers and the strength of alkali metal ion binding.

Proton Affinities. The preferred site of protonation to U is at the O4 position but results in greater structural perturbations than alkali metalation. The C═O−H^+ bond angle is 112.4° with the proton directed away from the adjacent N3H group and the direction of the permanent dipole moment. This indicates sp^2 hybridization, in contrast to the C═O−M^+ bond angles which are nearly linear and more akin to binding to the thioketo group. Three alternate and less stable proton binding sites are found with similar C═O−H^+ bond angles (Table 2). The second most favorable binding site is also at the O4 position with the proton directed toward the adjacent N3H group. Proton binding at this site is less favorable by 9.7 kJ/mol. The other two favorable binding sites are at the O2 position with the proton directed toward N3H being more favorable than toward N1H. Proton binding at these sites is less favorable than in the ground state O4 binding conformation by 29.9 and 34.7 kJ/mol, respectively. The results found for proton binding to the thiouracils are very similar to that found for U. In all cases thioketo or thioketo plus methyl substitution increases the proton affinity (PA) of all four sites by 0.1−38.2 kJ/mol. In contrast to alkali metal ion binding, the preferred site of protonation is always at the 4-position regardless of whether that corresponds to an oxygen or sulfur atom. In 2SU, 2-thioketo substitution results in only a small increase in the O4 PAs (<1 kJ/mol) and a much larger increase in the S2 PAs (21−24 kJ/mol) as compared to uracil. Methylation further enhances the PAs at all four sites. 5-Methylation enhances the O4 PAs by ∼7 kJ/mol and the S2 PAs by ∼15 kJ/mol, whereas 6-methylation enhances the O4 PAs by ∼18 kJ/mol and the S2 PAs by ∼12 kJ/mol as compared to 2SU. In contrast, 4-thioketo substitution results in only a small increase in the O2 PAs (<3 kJ/mol) and a much larger increase in the S4 PAs (15−24 kJ/mol) as compared to uracil. In 24SU the increase in the S2 and S4 PAs is fairly similar, ∼22−25 and 14−24 kJ/mol, respectively. These results clearly indicate that binding of protons by sulfur is more favorable than oxygen in contrast to that found for the alkali metal ions. This trend parallels that found for the isolated atoms, where sulfur is known to have a greater PA (664.3 kJ/mol) than oxygen (485.2 kJ/mol).[60,61] These trends also parallel those found in previous theoretical studies.[62−67]

Acidities. As one of the five commonly occurring nucleobases, uracil is often thought of in terms of its basic character; however, uracil exhibits acidic character as well. Substituents can alter the acidity of the N1−H and N3−H bonds and thereby affect its hydrogen bonding capabilities as well as the activities of enzymes for which uracil is a substrate.[1] To examine the influence of thioketo and thioketo plus methyl substitution on the acidity of uracil, theoretical computations were carried out

as described in the Theoretical Calculations section. The calculated gas-phase acidities of uracil and the thiouracils are summarized in Table 4. Also listed in Table 4 are literature values for the measured[68,69] and calculated acidities[62,68−71] of U, 2SU, 4SU, and 24SU. Our calculations find that the N1 position of uracil is considerably more acidic than the N3 position, by 49.4 kJ/mol. In previous work we also calculated the acidities of uracil at the CBS-Q level of theory.[34] Those calculations suggested that MP2 overestimates the N1 and N3 acidities of U but showed that the relative acidities were accurately reproduced. Thus, the trend in the MP2 acidities should be a good descriptor of the influence of thioketo or thioketo plus methyl substitution on the acidity of the N1 and N3 sites. The measured acidities of uracil also confirm that the N1 site is more acidic than the N3 site but by a greater difference than suggested by theory, 59 kJ/mol. Thioketo substitution leads to an increase in the acidity of both sites. 2-Thioketo substitution increases the acidity of the N3 site (25.6−31.8 kJ/mol) slightly more than that of the N1 site (21.7−27.0 kJ/mol). In contrast, 4-thioketo substitution increases the acidity of the N1 site (32.1 kJ/mol) slightly more than the N3 site (25.8 kJ/mol). Thioketo substitution at both the 2- and 4-positions produces a much greater increase in the N1 and N3 acidities, 53.5 and 50.7 kJ/mol, respectively.

Base Pairing. In nucleic acids uracil and thymine base pair with adenine via two hydrogen bonds in which the O4 and N3H atoms of U (T = 5MeU) interact with one of the amino H atoms and N1 of adenine (A), respectively. In the calculations performed here we only consider such Watson−Crick base pairing. The optimized structures of the A::U and A::SU base pairs are shown in Figure 6, while the hydrogen bond lengths and base pairing energies are summarized in Table 5. The base pairing energy of the A::U base pair is calculated to be 51.0 kJ/mol. Only a very small change in the base pairing energy is observed for the base pairs involving 2-thioketo substitution, A::2SU, A::5Me2SU, and 6Me2SU. The pairing energy increases by 0.2 and 0.3 kJ/mol for A::2SU and A::5Me2SU, respectively, and decreases by 0.1 kJ/mol for A::6Me2SU, as compared to the unsubstituted A::U base pair. This small change is not surprising because the sulfur substituent is not directly involved in the hydrogen bonding interactions, and therefore, only small changes in the geometry of these base pairs are found. The NH···O hydrogen bonds decrease in length from 0.032 to 0.039 Å while the N···HN hydrogen bonds increase in length from 0.066 to 0.067 Å in the A::2SU, A::5Me2SU, and A::6Me2SU base pairs as compared to the unsubstituted A::U base pair. In contrast, a significant decrease in the base pairing energy is observed for the base pairs involving 4-thioketo substitution. The pairing energy decreases by 4.0 and 10.7 kJ/mol for A::4SU and A::24SU, respectively, as compared to the unsubstituted A::U base pair. The large decrease in the pairing energy arises primarily because the C═S bonds in 4SU and 24SU are ∼0.4 Å longer than the C═O bonds. This difference leads to a significant change in the geometry of the base pair and a lengthening of both hydrogen bonds. The NH···S hydrogen bonds are 0.533 and 0.464 Å longer while the N···HN hydrogen bonds are 0.072 and 0.245 Å longer in the A::4SU and A::24SU base pairs, respectively, as compared to the corresponding hydrogen bonds in the unsubstituted A::U base pair. Similar trends, but less accurate energetics, for 2SU and 4SU were found in earlier theoretical studies.[72,73]

Alkali Metalated Base Pairing. Alkali metal ion binding to the A::2SU, A::4SU, and A::24SU base pairs was also examined. Four Na^+ binding sites were considered, binding at N3 or N7/NH_2 to A and O2 (S2) or O4(S4) binding to 2SU, 4SU, and 24SU. The N1 site of A was not considered as this is expected to be much less favorable because both hydrogen bonding interactions in the base pair would be disrupted by the metal-ion binding at this site. In addition, binding at this site would also result in significant puckering of the nucleotide backbone. Such puckering would lead to further losses in stability associated with disruption of the hydrogen bonding interactions in neighboring base pairs. Other alternative Na^+(A::SU) structures were not considered because the backbone of the nucleotide would not allow the bases to freely rotate to maximize the binding interactions with the sodium ion. In previous work the analogous Na^+(A::U) base pairs were also calculated.[34]

Alkali metal ion binding is found to increase the stability of the A::U and A::SU base pairs regardless of the binding site. Binding to A at N3 increases the pairing energy by 17.4 kJ/mol for the A::U base pair and by 23.6−29.9 kJ/mol for the A::SU base pairs. The increase in stability of the base pair likely arises as a result of the shortening of the N···HN hydrogen bond. Binding to A at the N7/NH_2 chelation site increases the pairing energy by 17.0 kJ/mol for the A::U base pair and by 19.5−23.9 kJ/mol for the A::SU base pairs. The increase in stability of the base pair upon binding at the N7/NH_2 site arises from the increased acidity of the amino hydrogen atom upon Na^+ binding. This is clearly seen as a shortening of the NH···O(S) hydrogen-bond length. Binding to U or SU at the O2(S2) position increases the pairing energy by 48.9 kJ/mol for the A::U base pair and by 40.4−64.1 kJ/mol for the A::SU base pairs. At first glance this is somewhat surprising as the length of both hydrogen bonds are observed to increase upon Na^+ binding. However, an additional metal chelation interaction with the N3 site of A occurs leading to stronger binding. Binding to U or SU at the O4(S4) position increases the pairing energy by 40.4 kJ/mol for the A::U base pair and by 42.5−71.3 kJ/mol for the A::SU base pairs. Again, this is somewhat surprising as Na^+ binding at this site disrupts the NH···O(S) hydrogen bond. However, additional chelation interactions with the amino nitrogen of A occur, leading to stronger binding. The effects are much larger for the A::4SU and A::24SU base pairs because Na^+ also gets close enough to N1 to achieve additional stabilization (Figure 3S).

When binding occurs at the N3 site, the base pairs remain planar and no additional chelation interactions occur. In all other cases Na^+ binding distorts the base pair from planarity. In the case of binding at N7, the base pairs distort only slightly from planarity to allow Na^+ to bind at the N7/NH_2 chelation site without loss of the hydrogen bonding interaction between the amino group and the O4(S4) positions. When binding occurs to U or SU at the O2(S2) or O4(S4) positions, the base pairs distort from planarity to allow Na^+ to interact with sites on both nucleobases, thereby stabilizing the base pairs through additional noncovalent interactions with the metal ion. Clearly the additional noncovalent interactions with the metal ion overcome the loss of stability associated with the nonideal hydrogen bonding geometries in these complexes.

Discussion

Comparison between Theory and Experiment. The alkali metal ion affinities of the thiouracils at 0 K measured by guided ion beam mass spectrometry and calculated here are summarized in Table 2. The agreement between theory and experiment is illustrated in Figure 8. It can be seen that the agreement is quite good for the Na^+(SU) and K^+(SU) complexes but less satisfactory for the Li^+(SU) complexes. The mean absolute deviations

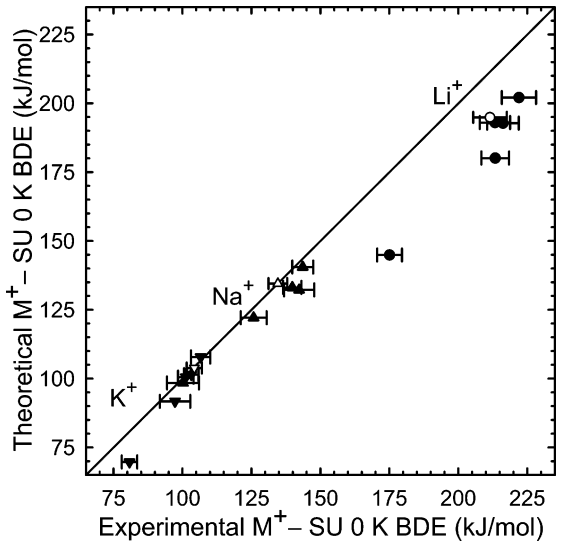

Figure 8. Theoretical versus experimental 0 K bond dissociation energies (in kJ/mol) of M^+(SU), where $M^+ = Li^+$ (○,●), Na^+ (△,▲), and K^+ (▽,▼) and SU = 2SU, 4SU, 24SU, 5Me2SU, and 6Me2SU. Previously measured values for U are shown as open symbols,[32] whereas values measured here for SU are shown as closed symbols.

(MAD) between experiment and theory for the Na^+(SU) and K^+(SU) systems are 4.0 ± 3.5 and 4.1 ± 4.4 kJ/mol, respectively, comparable to the average experimental uncertainty of 4.4 ± 1.3 kJ/mol. In contrast, the MAD for the Li^+(SU) complexes is much larger, 22.6 ± 6.3 kJ/mol. Theory systematically underestimates the BDEs for the Li^+(SU) complexes. This disparity may be a result of the higher degree of covalency in the Li^+−thiouracil interaction and suggests that this level of theory is inadequate for an accurate description of complexes to Li^+. Similar results have been found for a variety of ligands binding to Li^+.[32−34] Because such disparities have been observed for a wide variety of Li^+(ligand) complexes (including other nucleobases) previously investigated, this issue is the subject of another study being conducted in our laboratory. Preliminary results of this latter study suggest that the basis sets typically employed for Li^+ (including those employed in the present work) do not allow effective core polarization in the Li^+(ligand) complexes. Such core polarization appears to be very important for an accurate description of Li^+−ligand interactions, producing an enhancement in the binding interaction of approximately 10%, a value fairly similar to the underestimation of the Li^+−thiouracil BDEs measured here.

Conversion from 0 to 298 K. The 0 K BDEs determined here are converted to 298 K bond enthalpies and free energies. The enthalpy and entropy conversions are calculated using standard formulas and the vibrational and rotational constants determined for the MP2(full)/6-31G*-optimized geometries, which are given in Tables 1S and 2S. Table 4S lists 0 and 298 K enthalpy, free energy, and enthalpic and entropic corrections for all systems experimentally determined along with the corresponding theoretical values (Tables 1 and 2).

Trends in the Binding of Alkali Metal Ions to the Thiouracils. In all of the M^+(SU) systems the measured BDE varies with the metal ion such that Li^+ binds ∼60% more strongly than Na^+, which in turn binds ∼33% more strongly than K^+. Because these complexes are largely electrostatic in nature, this is easily understood based upon the size of the alkali metal ion. The smaller the ion, the shorter the metal−ligand distance and, therefore, the greater the strength of the ion−dipole and ion-induced dipole interactions. Simple correlations between the measured M^+−SU BDEs and the dipole moments or polarizabilities of these bases are not useful because the BDEs are also influenced by the alignment of the metal ion with the dipole moment and the nature of the donor atom (O versus S).

Theoretical examination of the Mulliken charges retained by the alkali metal ion shows that for the M^+(SU) complexes Li^+ retains less charge (0.60−0.73 e) than Na^+, which in turn retains less charge (0.74−0.97 e) than K^+ (0.87−0.99 e). These results confirm the electrostatic nature of the binding but also demonstrate that there is some covalency in the alkali metal ion−thiouracil interaction. The degree of covalency increases as the size of the alkali metal ion decreases such that $Li^+ > Na^+ > K^+$. The shorter the M^+−ligand bond distance, the more effectively the alkali metal ion is able to withdraw electron density from the neutral thiouracil and thus the charge retained by the alkali metal ion decreases. In addition, the charge retained by all three alkali metal ions is lower when the alkali metal ion binds to sulfur than when binding occurs to oxygen, indicating that the degree of covalency is greater for M^+−S than the corresponding M^+−O interactions. At first this result appears counterintuitive. However, sulfur is softer, more polarizable, and less electronegative than oxygen and thus more willing to donate electron density to the alkali metal ion, thereby resulting in more covalency in the M^+−S bonds.

Influence of Thioketo Substitution on the Alkali Metal Ion Binding Affinities of Uracil. As discussed above, variation in the M^+−SU BDEs with the alkali metal ion indicates that binding in these complexes is largely electrostatic. Therefore, the strength of the binding should be controlled by ion−dipole and ion-induced dipole interactions. The effect that thioketo or thioketo plus methyl substitution has upon binding can be examined by comparing these M^+(SU) systems to the corresponding M^+(U) systems. The strength of the ion−dipole interactions should correlate with the magnitude of the dipole moments of U and the SU nucleobases and the alignment of the alkali metal ion with the dipole moment vector in the M^+(U) and M^+(SU) complexes. As discussed above, in all cases thioketo or thioketo plus methyl substitution leads to an increase in the dipole moment of uracil. This would suggest that binding in all of the M^+(SU) complexes should be stronger than that in the M^+(U) complexes, which is clearly not the case. However, this conclusion ignores the alignment of the alkali metal ion with the dipole moment of the nucleobase, which becomes slightly poorer for all of the thiouracil complexes as compared to the uracil complexes, and other effects such as the polarizability and/or the position and nature of the donor atom. Thus, it is difficult to quantify whether the effects of the larger dipole moment or the poorer alignment with the dipole moment should dominate or if these essentially cancel each other. In any event, the relative alkali metal ion affinities of the thiouracils should follow the order U < 2SU ≈ 5Me2SU < 24SU < 4SU < 6Me2SU if the ion−dipole interactions are the dominant interaction in determining these trends. The strength of the ion-induced dipole interactions should correlate with the polarizability of the neutral thiouracil. The polarizability is not expect to vary significantly with the position of substitution, and the additivity method we used to estimate these polarizabilities is not sensitive to such structural differences. As summarized in Figure 1, the polarizability of uracil and the thiouracils follows the order U < 2SU ≈ 4SU < 5Me2SU ≈ 6Me2SU < 24SU. This suggests that if the ion-induced dipole interactions dominate the binding in these complexes, the M^+(U) and M^+(SU) BDEs should follow that same order. Clearly, this is not the case, suggesting that other factors dominate the binding. Careful examination of the trends in the alkali metal ion affinities of

the thiouracils shows that the nature of the donor atom cannot be ignored. Oxygen is clearly a better donor than sulfur, and of somewhat less importance, the 4-position is a better site for binding when the 2- and 4-positions are occupied by the same donor (both oxygen or sulfur). Taking these preferences into account and the relative dipole moments of the thiouracils provides a means by which the relative alkali metal ion BDEs can be understood. 24SU is the weakest binder because it only has sulfur donors. 4SU is the next weakest binder because binding must occur at O2. The binding to U, 2SU, and 5Me2SU is of very similar strength because the dipole moments do not vary significantly, while binding to 6Me2SU is the strongest because this ligand has the largest dipole moment.

Influence of Thioketo Substitution on the Proton Affinity of Uracil. The calculated PAs of uracil and the thiouracils are summarized in Table 2. In all cases thioketo and/or thioketo plus methyl substitution results in an increase in the PA of uracil. The relative PAs follow the order U $\approx$ 2SU < 5Me2SU < 4SU $\approx$ 24SU < 6Me2SU. The increase in the PA upon 2-thioketo substitution is very small ($\sim$0.1 kJ/mol), whereas a much larger increase is found for 4-thioketo substitution ($\sim$14−15 kJ/mol). This parallels the PAs of the binding site donor atoms, sulfur and oxygen as noted above. Methylation of 2SU leads to a further enhancement in the PA by 6.5 kJ/mol for 5Me2SU and 17.7 kJ/mol for 6Me2SU in accord with its affect on the dipole moments of these nucleobases. Also given in Table 2 are the measured PAs of U, 2SU, 4SU, and 24SU.[61,63,64] In contrast to theory, the measured PAs follow the order U < 2SU < 4SU < 24SU. The experimental results agree with theory in that 2-thioketo substitution has a smaller effect on the PA than 4-thioketo substitution but suggest that thioketo substitution significantly impacts the PA even when the proton is not bound to that site.

Influence of Thioketo Substitution on the Acidity of Uracil. The calculated acidities of uracil and the thiouracils are summarized in Table 4. Also given in Table 4 are literature values for the measured[68,69] and calculated[34,62,68−71] acidities of U as well as the calculated acidities of 2SU, 4SU, and 24SU.[62] In all cases thioketo substitution results in an increase in the acidity of uracil that is only mildly dependent upon the position of substitution, but strongly dependent upon the extent of substitution. 2-Thioketo substitution increases the acidity of uracil by 27.0 kJ/mol, whereas the effect of 4-thioketo substitution is somewhat greater and results in a 32.1 kJ/mol increase in the acidity. The effects of dithioketo substitution are nearly additive such that the acidity of 24SU increases by 53.5 kJ/mol as compared to U. Methylation of 2SU leads to a small decrease ($\sim$3−6 kJ/mol) in the acidity regardless of the position of substitution. Because sulfur is larger and more polarizable than oxygen, the deprotonated anions of the thiouracils will be more stable than those for uracil because the negative charge is spread over a larger volume. This simple explanation suggests that the position of substitution is not very important in determining the acidity. Dithioketo substitution increases the volume or decreases the charge density of the deprotonated anion even further and thus leads to an even greater enhancement in the acidity. Methylation decreases the acidity because the methyl substituents are electron donating. Methylation therefore leads to greater electron density in the aromatic ring, thereby destabilizing the deprotonated anion and reducing the acidity.

Implications for Nucleic Acid Stability. The present results allow predictions for metal-induced and thioketo-substitution-induced stability changes in nucleic acids. In previous work we examined the metal-induced stability changes by examining the influence of binding Na^+ to the A::U base pair.[32] We extend that work to include Na^+ binding to the A::2SU, A::4SU, and A::24SU base pairs. Binding of Na^+ to the O2(S2) and O4(S4) sites of the base pairs is found to be more favorable than binding to the N7/NH2 and N3 sites of A. In addition, binding of Na^+ to the base pairs is found to increase the pairing energy by 17.0−71.3 kJ/mol and therefore suggests that alkali metal cationization should increase the stability of nucleic acids. However, alkali metal cationization causes the base pairs to distort from planarity and could weaken hydrogen bonding interactions between nearby base pairs. This would reduce the stabilization gained from the additional chelation interactions with the alkali metal ion and impact the stability of the nucleic acid to a lesser extent than for the isolated base pair. These effects are slightly larger for 2SU and even larger for 4SU and 24SU, which contrast the trends in the alkali metal ion binding affinities for the isolated nucleobases. The presence of the alkali metal ion would also tend to increase the strength of base stacking interactions via cation−π interaction of the alkali metal ion with the adjacent nucleobases. Thioketo substitution at either the 2- or 4-position should lead to a small increase in the strength of the stacking interactions as a result of the enhanced polarizability. Thus, alkali metal ion binding to thiouracil nucleobases should increase the stability of nucleic acids by reducing the charge on the nucleic acid via a zwitterion effect as well as through additional noncovalent interactions between the alkali metal ion and the nucleobases and stacking interactions between the bases.

As discussed above, thioketo substitution alters many properties of uracil, e.g., dipole moment, polarizability, acidity, basicity, and its interactions with alkali metal ions. The enhanced acidity of the N1H position would tend to decrease the stability of thioketo-substituted nucleic acids, making the base more susceptible to cleavage of the glycosidic bond. The N1 hydrogen is also lost during RNA formation, and therefore, the enhanced N1H acidity might facilitate this process and also affect the dynamics of DNA transcription. During the transcription of DNA U and A comprise the base pairs. It is known that the stability of DNA is controlled by the strength of hydrogen bonding in the base pairs as well as stacking interactions between adjacent base pairs. In double-stranded DNA thymine base pairs with adenine via two hydrogen bonds in which the O4 and N3H atoms of T interact with one of the amino H atoms and N1 of A, respectively. The strength of hydrogen bonding in the A::U (A::T) base pairs is controlled by the acidity of N3H and the PA of the less favorable O4 (S4) binding site. The increase in the PA of this site upon thioketo substitution would tend to strengthen the hydrogen bonding interactions in the A::SU base pairs. Likewise, the greater acidity of the N3H position would tend to make this site a better proton donor, resulting in stronger hydrogen bonding interactions. Overall these effects might be expected to stabilize base pairing for the 2-thioketo-substituted uracils and lead to a small increase in the stability of the A::SU base pairs. However, this effect is quite small as the calculated enhancement in the base pairing energy for the 2-thioketo-substituted uracils is <1 kJ/mol. These effects might also be expected to stabilize base pairing for the 4-thioketo-substituted uracils. However, the longer C═S bond leads to significant distortion of the A::SU base pair and a decrease in the pairing energy.

Theoretical studies[74,75] have shown that in DNA the stacking interaction between the nucleobases is mainly controlled by dispersion energy, which is proportional to the polarizabilities of the interacting molecules. These studies[74,75] also concluded that the nucleobases stack in the antiparallel direction of the

dipole moments as a result of dipole−dipole interactions between nucleobase pairs. Because thioketo substitution alters the magnitude and direction of the dipole moment as well as the polarizability of U, these changes might induce minor conformational changes in DNA and alter the strength of the stacking interactions, both of which are likely to produce additional effects upon their functions as suggested by previous studies. These effects are expected to be somewhat smaller for 2-thioketo-substituted uracils than 4-thioketo-substituted uracils because the sulfur substituent is directly involved in the hydrogen bonding interactions and the changes in the magnitude and direction of the dipole moment are more significant in the latter species.

Conclusions

The kinetic-energy dependence of the collision-induced dissociation of M^+(SU), where $M^+ = Li^+$, Na^+, and K^+ and SU = 2-thiouracil, 4-thiouracil, 2,4-dithiouracil, 5-methyl-2-thiouracil, and 6-methyl-2-thiouracil, with Xe are examined in a guided ion beam mass spectrometer. The dominant dissociation process is loss of the intact neutral thiouracil. Thresholds for these processes are determined after consideration of the effects of reactant internal energy, multiple collisions with Xe, and dissociation lifetime. Insight into the structures and binding of alkali metal ions to the thiouracils as well as the effects of thioketo substitution on the proton affinities, acidities, and base pairing energies is provided by ab initio calculations. Very good agreement between the experimentally determined and theoretically calculated alkali metal ion affinities is obtained for the Na^+(SU) and K^+(SU) complexes, suggesting that these ligands can act as reliable anchors for the alkali metal ion affinity scales and broaden the range of ligands available as absolute thermochemical anchors. The calculated BDEs for the Li^+(SU) complexes are found to be systematically lower than the values measured here. These discrepancies are not completely understood but appear to be a result of several subtle electronic effects that require the use of basis sets that allow core penetration to accurately predict the BDEs in the Li^+(SU) systems. Further, the combined experimental and theoretical results provide an understanding of the influence of alkali metal ion binding and thioketo substitution on the structure and stability of nucleic acids. Alkali metal ion binding is expected to increase the stability of both single-stranded and double-stranded nucleic acids by reducing the charge on the nucleic acid in a zwitterion effect as well as through additional noncovalent interactions between the alkali metal ion and the nucleobases. Thioketo substitution is found to further influence the stability of nucleic acids by increasing the proton affinity and acidity of uracil. The effect of thioketo substitution on the alkali metal ion binding affinity as well as the stability of the A::U base pair is dependent upon the position of substitution. 2-Thioketo substitution leads to an increase in both the alkali metal ion binding affinity and the base pairing energy, whereas 4-thioketo substitution leads to a decrease in both. The latter differences in the effects of 2- versus 4-thioketo substitution may explain why 2-thioketo-substituted uracils are found more often in nature than 4-thioketo-substituted uracils.

Acknowledgment. This work is supported by the National Science Foundation, Grant CHE-0518262.

Supporting Information Available: Tables of vibrational frequencies, average vibrational energies, rotational constants, optimized geometries of SU, M^+(SU), and A::SU base pairs, and enthalpies and free energies of M^+ binding to SU; figures showing cross sections for the collision-induced dissociation of M^+(SU) with Xe as well as empirical fits to the M^+ product channels, where $M^+ = Li^+$, Na^+, and K^+ and SU = 4SU, 24SU, 5Me2SU, and 6Me2SU, and optimized geometries of Na^+X-(SU) base pair complexes, where X = N3, N7/NH_2, O2(S2), and S4 and SU = 4SU and 24SU. This material is free of charge via the Internet at http://pubs.acs.org

References and Notes

(1) Saenger, W. *Principles of Nucleic Acid Structure*; Springer-Verlag: New York, 1984; Chapter 7.
(2) Yaniv, M.; Folk, W. R. *J. Biochem.* **1975**, *250*, 3243.
(3) Jeffrey, G. A.; Saenger, W. *Hydrogen Bonding in Biological Structures*; Springer: New York, 1991.
(4) Beck, C. F.; Howlett, G. *J. Mol. Biol.* **1977**, *111*, 1.
(5) Miller, W. H.; Robin, R. O.; Astwood, E. B. *J. Am. Chem. Soc.* **1945**, *67*, 2201.
(6) Willams, R. H.; Bissel, G. W. *Science* **1968**, *98*, 156.
(7) Ortiga-Carvalho, T. M.; Hashimoto, K.; Pazos-Moura, C. C.; Geenen, D.; Cohen, R.; Lang, R. M.; Wondisford, F. E. *Endocrinology* **2004**, *145*, 1625.
(8) Gredilla, R.; Barja, G.; Lopez-Torres, M. *Free Radical Res.* **2001**, *35*, 417.
(9) Palumbo, A.; d'Ishia, M. *Biochem. Biophys. Res. Commun.* **2001**, *282*, 793.
(10) Sułkowska, A.; Równicka, J.; Bojko, B.; Sułkowski, W. *J. Mol. Struct.* **2003**, *651*, 133.
(11) Theodossiou, C.; Schwarzenberger, P. *Am. J. Med. Sci.* **2000**, *319*, 96.
(12) Macchia, M.; Barontini, S.; Bertini, S.; Di Bussolo, V.; Forli, S.; Giovannetti, E.; Grossi, E.; Minutolo, F.; Danesi, R. *J. Med. Chem.* **2001**, *44*, 3994.
(13) Elias, A. N. *Med. Hypotheses* **2004**, *62*, 431.
(14) Antoniadis, C. D.; Corban, G. J.; Hadjikakou, S. K.; Hadjiliadis, N.; Kubicki, M.; Warner, S.; Butler, I. S. *Eur. J. Inorg. Chem.* **2003**, *8*, 1635.
(15) Imam, D. R.; El-Barbary, A. A.; Nielsen, C.; Pedersen, E. B. *Monatsh. Chem.* **2002**, *133*, 723.
(16) Abdel-Rahman, A. A. H.; Abdel-Megied, A. E. S.; Goda, A. E. S.; Zeid, I. F.; El Ashry, E. S. H. *Nucleosides Nucleotides* **2003**, *22*, 2027.
(17) Inazumi, M.; Kano, F.; Sakata, S. *Chem. Pharm. Bull.* **1992**, *40*, 1808.
(18) Castillo, J.; Benavente-Garcia, O.; Lorente, J.; Alcaraz, M. J.; Redondo, A.; Ortuno, A.; Del Rio, J. A. *J. Agric. Food Chem.* **2000**, *48*, 1738.
(19) Kamalakannan, P.; Venkappayya, D. *J. Inorg. Biochem.* **2002**, *90*, 22.
(20) Kamalakannan, P.; Venkappayya, D. *Russ. J. Coord. Chem.* **2002**, *28*, 423.
(21) Lippard, S. J. *Acc. Chem. Res.* **1978**, *11*, 211.
(22) Misztal, G.; Przyborowski, L. *Ann. Univ. Mariae Curie Sklodowska* **1983**, *38*, 135.
(23) Pearson, R. G. *Science* **1966**, *151*, 172.
(24) Ahrland, S.; Chatt, J. Davise, N. K. *Q. Rev. Chem. Soc.* **1958**, *12*, 265.
(25) Eichhorn, G. L. *Adv. Inorg. Biochem.* **1981**, *3*, 1.
(26) Shack, J.; Jenkins, R. J.; Thompsett, J. M. *J. Biol. Chem.* **1953**, *203*, 373.
(27) Dove, W. F.; Davidson, N. *J. Mol. Biol.* **1962**, *5*, 467.
(28) Eichhorn, G. L. *Nature* **1962**, *194*, 474.
(29) Eichhorn, G. L.; Shin, Y. A. *J. Am. Chem. Soc.* **1968**, *90*, 7323.
(30) Ruddo, N.; Toscano, M.; Grand, A. *J. Am. Chem. Soc.* **2001**, *123*, 10272.
(31) Shin, Y. A.; Eichhorn, G. L. *Biopolymers* **1977**, *16*, 225.
(32) Rodgers, M. T.; Armentrout, P. B. *J. Am. Chem. Soc.* **2000**, *122*, 8548.
(33) Yang, Z.; Rodgers, M. T. *J. Am. Chem. Soc.* **2004**, *126*, 16217.
(34) Yang, Z.; Rodgers, M. T. *Int. J. Mass Spectrom.* **2005**, *241*, 225.
(35) Rodgers, M. T.; Armentrout, P. B. *J. Am. Chem. Soc.* **2002**, *124*, 2678.
(36) Ruan, C.; Rodgers, M. T. *J. Am. Chem. Soc.* **2004**, *126*, 14600.
(37) Rannulu, N.; Rodgers, M. T. *Phys. Chem. Chem. Phys.* **2004**, *7*, 2749.
(38) Miller, K. J. *J. Am. Chem. Soc.* **1990**, *112*, 8533.
(39) Rodgers, M. T.; Ervin, K. M.; Armentrout, P. B. *J. Chem. Phys.* **1997**, *106*, 4499.
(40) Rodgers, M. T. *J. Chem. Phys. A* **2001**, *11*, 2374.
(41) Muntean, F.; Armentrout, P. B. *J. Chem. Phys.* **2001**, *115*, 1213.

(42) Dalleska, N. F.; Honma, K.; Armentrout, P. B. *J. Am. Chem. Soc.* **1993**, *115*, 12125.
(43) Aristov, N.; Armentrout, P. B. *J. Phys. Chem.* **1986**, *90*, 5135.
(44) Hales, D. A.; Armentrout, P. B. *J. Cluster Sci.* **1990**, *1*, 127.
(45) Teloy, E.; Gerlich, D. *Chem. Phys.* **1974**, *4*, 417. Gerlich, D. Diplomarbeit, University of Freiburg, Federal Republic of Germany, 1971. Gerlich, D. In *State-Selected and State-to-State Ion−Molecule Reaction Dynamics, Part I, Experiment*; Ng, C.-Y., Baer, M., Eds.; Advances in Chemical Physics series; Wiley: New York, 1992; Vol. 82, p 1.
(46) Rodgers, M. T.; Armentrout, P. B. J. *Phys. Chem. A* **1997**, *101*, 2614.
(47) Ervin, K. M.; Armentrout, P. B. *J. Chem. Phys.* **1985**, *83*, 166.
(48) Hales, D. A.; Lian, L.; Armentrout, P. B. *Int. J. Mass Spectrom. Ion Processes* **1990**, *102*, 269.
(49) Frisch, M. J.; Trucks, G. W.; Schlegel, H. B.; Scuseria, G. E.; Robb, M. A.; Cheeseman, J. R.; Zakrzewski, V. G.; Montgomery, J. A., Jr.; Stratmann, R. E.; Burant, J. C.; Dapprich, S.; Millam, J. M.; Daniels, A. D.; Kudin, K. N.; Strain, M. C.; Farkas, O.; Tomasi, J.; Barone, V.; Cossi, M.; Cammi, R.; Mennucci, B.; Pomelli, C.; Adamo, C.; Clifford, S.; Ochterski, J.; Petersson, G. A.; Ayala, P. Y.; Cui, Q.; Morokuma, K.; Malick, D. K.; Rabuck, A. D.; Raghavachari, K.; Foresman, J. B.; Cioslowski, J.; Ortiz, J. V.; Baboul, A. G.; Stefanov, B. B.; Liu, G.; Liashenko, A.; Piskorz, P.; Komaromi, I.; Gomperts, R.; Martin, R. L.; Fox, D. J.; Keith, T.; Al-Laham, M. A.; Peng, C. Y.; Nanayakkara, A.; Gonzalez, C.; Challacombe, M.; Gill, P. M. W.; Johnson, B.; Chen, W.; Wong, M. W.; Andres, J. L.; Gonzalez, C.; Head-Gordon, M.; Replogle, E. S.; Pople, J. A.; *Gaussian 98*, Revision A.11; Gaussian, Inc.: Pittsburgh, PA, 1998.
(50) *Exploring Chemistry with Electronic Structures Methods*, 2nd ed.; Foresman, J. B., Frisch, Æ., Eds.; Gaussian: Pittsburgh, PA, 1996.
(51) Boys, S. F.; Bernardi, R. *Mol. Phys.* **1979**, *19*, 553.
(52) Van Duijneveldt, F. B.; van Duijneveldt-van de Rijdt, J. G. C. M.; van Lenthe, J. H. *Chem. Rev.* **1994**, *94*, 1873.
(53) Beyer, T. S.; Swinehart, D. F. *Comm. Assoc. Comput. Mach.* **1973**, *16*, 379. Stein, S. E.; Rabinovitch, B. S. *J. Chem. Phys.* **1973**, *58*, 2438; *Chem. Phys. Lett.* **1977**, *49*, 1883.
(54) Pople, J. A.; Schlegel, H. B.; Raghavachari, K.; DeFrees, D. J.; Binkley, J. F.; Frisch, M. J.; Whitesides, R. F.; Hout, R. F.; Hehre, W. J. *Int. J. Quantum Chem. Symp.* **1981**, *15*, 269. DeFrees, D. J.; McLean, A. D. *J. Chem. Phys.* **1985**, *82*, 333.
(55) Khan, F. A.; Clemmer, D. E.; Schultz, R. H.; Armentrout, P. B. *J. Phys. Chem.* **1993**, *97*, 7978.
(56) Chesnavich, W. J.; Bowers, M. T. *J. Phys. Chem.* **1979**, *83*, 900.
(57) Armentrout, P. B. In *Advances in Gas-Phase Ion Chemistry*; Adams, N. G., Babcock, L. M., Eds.; JAI: Greenwich, 1992; Vol. 1, pp 83−119.
(58) Armentrout, P. B.; Simons, J. *J. Am. Chem. Soc.* **1992**, *114*, 8627.
(59) Figures were generated using the output of Gaussian 98 geometry optimizations in Hyperchem Computational Chemistry Software Package, Version 5.0, Hypercube Inc., 1997.
(60) NIST Standard Reference Database. Hunter, E. P.; Lias, S. G. Gas Phase Ion Energy Data. In *NIST Chemistry WebBook*; Linstrom, P. J., Mallard, W. G., Eds.; NIST Standard Reference Database Number 69; National Institute of Standards and Technology: Gaithersburg MD, June 2005 (http://webbook.nist.gov).
(61) Hunter, E. P.; Lias, S. G. Evaluated Gas-Phase Basicities and Proton Affinities of Molecules: An Update. *J. Phys. Chem. Ref. Data* **1998**, *27*, 3, 413−656.
(62) Kryachko, E.; Nguyen, M. T.; Zeegers-Huyskens, T. *J. Phys. Chem. A* **2001**, *105*, 3379.
(63) Lamsabhi, M.; Alcamí, M.; Mó, O.; Bouab, W.; Esseffar, M.; Abboud, J. L.-M.; Yáñez, M. *J. Phys. Chem. A* **2000**, *104*, 5122.
(64) Kurinovich, M. A.; Phillips, L. M., Sharma, S.; Lee, J. K. *Chem. Commun*. **2002**, 2354.
(65) Wolken, J. K.; Tureček, F. *J. Am. Soc. Mass Spectrom*. **2000**, *11*, 1065.
(66) Podolyan, Y.; Gorb, L.; Leszczynski, J. *J. Phys. Chem. A* **2000**, *104*, 7346.
(67) Moustafa, H.; El-Taher, S.; Shibl, M. F.; Hilal, R. *Int. J. Quantum Chem.* **2002**, *87*, 378.
(68) Kurinovich, M. A.; Lee, J. K. *J. Am. Chem. Soc.* **2000**, *122*, 6258.
(69) Miller, T. M.; Arnold, S. T.; Viggiano, A. A.; Stevens Miller, A. E. *J. Phys. Chem. A* **2004**, *108*, 3439.
(70) Nguyen, M. T.; Chandra, A. K.; Zeegers-Huyskens, T. *J. Chem. Soc., Faraday Trans*. **1998**, *94*, 1277.
(71) Huang, Y.; Kenttämaa, H. *J. Phys. Chem. A* **2003**, *107*, 4893.
(72) Eriksson, L. A.; Kryachko, S.; Nguyen, M. T. *Int. J. Quantum Chem*. **2004**, *99*, 841.
(73) Šponer, J.; Leszcyński, J.; Hobza, P. *J. Phys. Chem. A* **1997**, *101*, 9489.
(74) Hobza, P.; Šponer, J.; Polášek, M. *J. Am. Chem. Soc*. **1995**, *117*, 792.
(75) Šponer, J.; Leszcyński, J.; Hobza, P. *J. Phys. Chem*. **1996**, *100*, 5590.